Conference materials
UDC 548.73
DOI: https://doi.org/10.18721/JPM.161.125

Study of defects in shaped sapphire crystals by synchrotron X-ray phase contrast imaging

T.S. Argunova [1]✉, V.G. Kohn [2], V.M. Krymov [1]

[1] Ioffe Institute, St. Petersburg, Russia;

[2] National Research Centre "Kurchatov Institute", Moscow, Russia

✉argunova@mail.ioffe.ru

Abstract. Single crystalline sapphire ribbons grown by the Stepanov method exhibit relatively high dislocation densities and often contain slightly misoriented grains. In order to understand the formation of dislocation structures during growth, we studied neck portions cut off perpendicular to the growth axis [$\bar{1}$010] of basal-plane-faceted ribbons. The samples have been characterized using phase-contrast and Bragg-diffraction imaging (topography) with synchrotron radiation. It has been found that in the growth direction from the neck towards the main body of the ribbon the dislocation density increases due to multiplication of dislocations. Combining the both imaging techniques, the dislocations were shown to be located around gas voids in sapphire crystals. Computer simulations of the phase-contrast images were carried out to obtain the correct size of the voids.

Keywords: synchrotron phase contrast imaging, computer simulations, shaped sapphire

Funding: This study was funded by Russian Foundation for Basic Research (RFBR), grant numbers 19-29-12041 mk and 19-29-12043 mk.

Citation: Argunova T.S., Kohn V.G., Krymov V.M., Study of defects in shaped sapphire crystals by synchrotron X-ray phase contrast imaging, St. Petersburg State Polytechnical University Journal. Physics and Mathematics. 16 (1.1) (2023) 146–152. DOI: https://doi.org/10.18721/JPM.161.125

This is an open access article under the CC BY-NC 4.0 license (https://creativecommons.org/licenses/by-nc/4.0/)

Материалы конференции
УДК 548.73
DOI: https://doi.org/10.18721/JPM.161.125

Исследование дефектов в профилированных кристаллах сапфира методом фазово-контрастного изображения в синхротронном излучении

Т.С. Аргунова [1]✉, В.Г. Кон [2], В.М. Крымов [1]

[1] Физико-технический институт им. А.Ф. Иоффе РАН, Санкт-Петербург, Россия;

[2] Национальный исследовательский центр "Курчатовский институт", г. Москва, Россия

✉ argunova@mail.ioffe.ru

Аннотация. Способом Степанова выращивают изделия из сапфира (α-Al_2O_3) контролируемых размеров и формы. Исследование дефектов в профилированном сапфире проводилось путем совместного использования методов фазово-контрастного изображения и топографии в синхротронном излучении. Взаимодополняющий характер методов, состоящий в том, что метод фазового контраста выявляет размер газового включения, а топограмма показывает дислокации решетки, позволил охарактеризовать концентраторы напряжений и провести анализ типов дислокаций. Таким образом, нами решена задача определения размеров газовых микровключений и выявлена их роль в формировании дислокационных ансамблей.

© Argunova T.S., Kohn V.G., Krymov V.M., 2023. Published by Peter the Great St. Petersburg Polytechnic University.

Ключевые слова: синхротронное излучение, фазово-контрастное изображение, компьютерное моделирование, профилированный сапфир

Финансирование: Работа выполнена при поддержке Российского Фонда Фундаментальных Исследований (РФФИ), гранты № 19-29-12041 мк и № 19-29-12043 мк.

Ссылка при цитировании: Аргунова Т.С., Кон В.Г., Крымов В.М., Исследование дефектов в профилированных кристаллах сапфира методом фазово-контрастного изображения в синхротронном излучении // Научно-технические ведомости СПбГПУ. Физико-математические науки. 2023. Т. 16. № 1.1. С. 146–152. DOI: https://doi.org/10.18721/ JPM.161.125

Статья открытого доступа, распространяемая по лицензии CC BY-NC 4.0 (https://creativecommons.org/licenses/by-nc/4.0/)

Introduction

Shaped sapphire crystals are produced by melt crystallization. Originally developed by Stepanov and named after him, the shaped crystal growth method was extended by LaBelle, Chalmers, et al. The crystallization was described as edge-defined, film-fed growth (EFG) process. A variety of instruments based on many sizes and shapes of sapphire, including tubes, rods, needles, and filaments are profitably used in optical, medical, and electrical devices (see, e.g., review [1]). In addition, EFG single-crystal plates of large diameter were produced to meet the objectives of Light Emitting Diodes (LEDs) market [2]. Nevertheless, sapphire ribbons with large {0001} basal faces are not suitable for mass production of LED substrates due to structural defects [3]. Conventionally grown sapphire windows have the wide front side surface of the prismatic orientation $\{11\bar{2}0\}$.

Crystals grown from a gas-saturated melt usually contain gas inclusions, or voids. The gas voids are formed due to the entrapment of gas bubbles that originate in the vicinity of the melt-solid interface. The distribution of the voids was found to depend on a number of parameters. By controlling the pulling rate, a stability of the melt meniscus, a design of the shaper, *etc*., a reduction in the number of the voids is achieved [4]. In practice, the complete removal of voids hardly ever occurs in shaped sapphire growth processes.

Gas voids in sapphire ribbons seriously deteriorate the crystal quality and hence the application of these products. X-ray Bragg diffraction topography was used to visualize structural defects and voids in basal-plane-faceted ribbons [5]. As a result, an increase in the dislocation density near the voids indicated that the voids initiated dislocations. However, the dislocation density was too high to allow an analysis of the types and a quantification of the number of dislocations in the bulk of the crystal. The proposed model explained the formation of a block structure [5], but knowledge regarding stress concentrators was very limited.

The purpose of this paper was to partially fill these gaps. In a strongly deformed region around the generation source of dislocations, the x-ray topographic images of the source and individual dislocations superimpose and are no longer distinguishable. Therefore we decided to take advantage of the properties of a third-generation synchrotron radiation (SR) beam and use the in-line phase-contrast imaging (PCI) method [6]. The transverse coherence length of SR beams typically equals 30–50 μm, while it is less than 1 μm for usual laboratory sources. A partially coherent SR beam makes it possible to visualize μm-sized inhomogeneities by the total phase shift along the beam path. In the case of sapphire, negligible absorption when working in the 16–22 keV range produces no absorption contrast from a microvoid. However, phase contrast appears if the detector is moved away from the sample. The objectives of the article were to detect the microvoids and study the extent to which their size and shape are described by the PCI.

Materials and Methods

Phase-contrast imaging

A basal-plane-faceted ribbon 31×1.3×265 ($W \times H \times L$) mm^3 was grown by the Stepanov/EFG method. The growth process took place in a specially designed thermal zone where heat shields were used. The growth rate was 1 mm × min^{-1}. The wide as-grown surfaces of the ribbon were

© Аргунова Т.С., Кон В.Г., Крымов В.М., 2023. Издатель: Санкт-Петербургский политехнический университет Петра Великого.

smooth and mirror-like. Laser adjustment of the seed relative to the pulling device and shaper allowed us to achieve high orientation accuracy. The misorientation of the surface relative to the basal face was several arc minutes. A 1 mm thick sample with a neck was cut out along the $[\bar{1}2\bar{1}0]$ direction from the neck portion of the ribbon. Preliminary characterization of the ribbon surfaces using optical microscopy showed that the sample did not contain blocks. The formation of blocks began at a distance of about 200 mm from the seed. The scheme of the ribbon orientation and the sample is shown in Fig. 1.

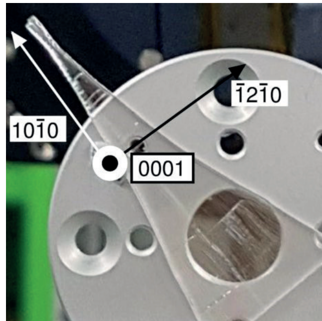

Fig. 1. Neck portion of sapphire ribbon

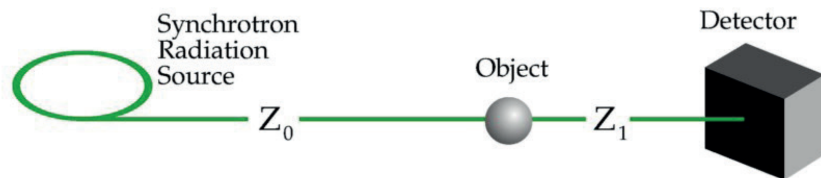

Fig. 2. Schematic display of the experimental setup for phase-contrast imaging. Object thickness $t << Z_1 << Z_0$

Fig. 2 schematically represents the principle of in-line phase-contrast imaging. The sample is illuminated by a synchrotron x-ray beam monochromated to a wavelength λ. Due to the large source–to–sample distance Z_0 and the small size σ of the source, a highly spatial coherent beam is produced. In such a condition, the transverse coherence length, given by the relation $d = \lambda Z_0/2\sigma$, results to be at least several tens of micrometers. A CCD detector is placed at distance Z_1 from the sample, typically in the range from a few centimeters to about a meter. It is known that in the near-field region of object–to–detector distances, the transverse dimension of, say, a pore can be determined from image pixels (measured directly on images), provided that the detector resolution is satisfactory. The near-field condition is fulfilled for $2r_1 << D$, where $r_1 = (\lambda Z_1)^{1/2}$ is the radius of the first Fresnel zone at a distance Z_1 from a void of size D. Note that if D were a few microns, then the correct estimate for the distance Z_1, where the actual size correlates with the image size, would be about 10 times smaller than Z_c, where Z_c corresponds to $r_1 = D/2$. For a micropipe as an example, $Z_1 = 0.1$ cm with a micropipe diameter $D = 2$ μm and λ = 0.775 Å [7]. This means that the image must be recorded very close to the sample, when Z_1 is in the millimeter range. Moving further from the sample towards the far-field region, where $2r_1 >> D$, the image size is increased and many Fresnel zones are formed. One can find the real size from the phase shift of x-rays transmitting through an object by recording images at multiple distances and solving the inverse problem.

Experiments were performed at the Pohang Light Source (PLS), Pohang, South Korea, at a beamline devoted to imaging. PLS operates at 3 GeV with an emittance of 12 μm×rad. 6C imaging beamline is characterized by a small vertical size of the source σ: 495(H)×29(V) μm^2 and a large source–to–sample distance L (36 m). The broad spectrum of wavelengths provided by the multi-pole wiggler was monochromated by two parallel silicon crystals with reflection 111. The energy resolution was $\Delta E/E \approx 10^{-4}$. The actual photon energy was $E = 25$ keV. The Zyla CCD camera (Andor, Oxford Instruments, UK) had 2560×2160 pixel resolution and 6.5×6.5 μm^2 pixel size. Therefore the maximal sample area (the field of view, FOV) that a camera could image was 16.6×14.0 mm^2. Image recording was preceded by a conversion step in which the LuAG:Ce scintillator converted radiation into light. An optical lens served as the coupling element between the scintillator and the CCD. The lens affected the FOV size and image resolution.

Note that the PCI technique differs from X-ray microscopy in that PCI does not use focusing optics. Hence, a wide partially coherent SR beam makes it possible to image microvoids in the entire volume of large and rather thick samples. At the same time, a magnifying lens allows high-resolution imaging with medium-resolution detectors. When a visible light image is magnified by 20 ×, the pixel-to-object size ratio decreases. Formally speaking, the effective pixel size is reduced from 6.5 to 0.32 μm.

X-ray topography

Crystal defects such as dislocations were visualized using Bragg-diffraction imaging (X-ray topography, XRT). A multilayer mirror with an energy resolution of $\Delta E/E \approx 2\%$ at 15 keV provided a monochromatic beam by using vertical projection of the source. Typical exposure times were short due to high intensity available at the PLS 6C wiggler beamline. They ranged from several tens of seconds (on the fine-grain film Kodak M100) to several seconds (on the detector). High-speed images were recorded on a large view field (64×42 mm^2) detector (VHR CCD, Photonic Science, UK) with a pixel pitch of 16 μm.

Comparison of PC and XRT images could not be performed within the same experimental session due to differences in setups and viewing angles. Nevertheless, PC images were recorded when the sample was set in the azimuth position for Laue diffraction.

Results

Figure 3 shows X-ray topographs taken on film (*a*) and CCD (*b*). The topographs were acquired from the region located near the beginning of the sapphire ribbon. The high-speed CCD image visualizes structural features distributed over a large sample area. At a distance of approximately 15 mm from the crystal neck generation sources of dislocations can be observed. The sources and nearby dislocations form rows in mutually orthogonal directions: along and across the ribbon growth. The numbers 1–4 indicate the longitudinal rows. Among the transverse ones, rows 5 and 6 are closest to the neck.

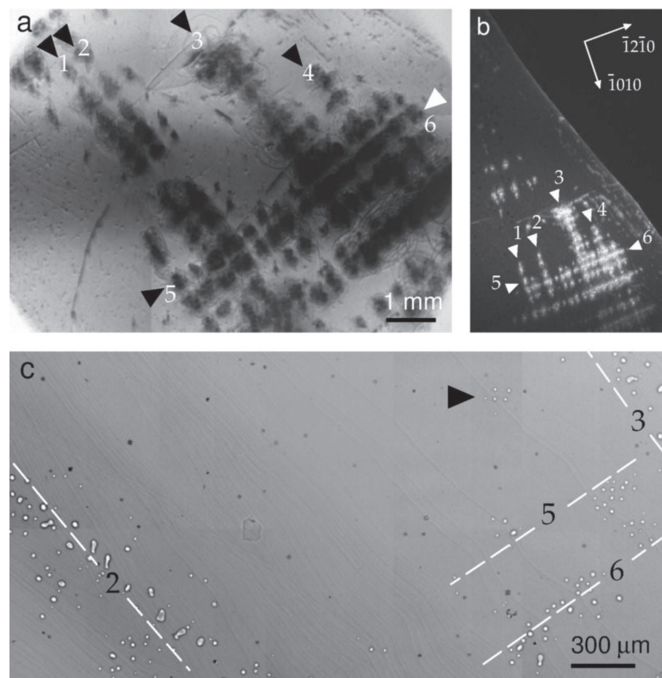

Fig. 3. Synchrotron X-ray topographs of dislocations in sapphire in reflections 1120 (*a*) and 000.18 (*b*). E = 15 keV. The diffraction vector is directed from bottom to top (*c*). Phase-contrast images combined together to map the area shown in (*a*)

Note that X-ray topography is well suited for observing defects like dislocations and inclusions in high-quality sapphire crystals. But in the case of very high local concentration of dislocations, the images of individual defects are superimposed. This is the case of the ribbon shown in Fig. 3. Therefore, in order to observe the generation sources separately from dislocations, we decided to take advantage of the PCI method.

The sources of dislocations are unevenly distributed over the area of the sample. The voids in the phase-contrast image are arranged in a similar way. Their dense distribution in the longitudinal (2, 3) and transverse (5, 6) directions is shown by dashed lines in Fig. 3, *c*. A direct comparison of the topographs and the phase-contrast image reveals the relationship between dislocations nucleated in the ribbon and gas voids.

Several features are apparent in Fig. 3. Firstly, the dislocation density changes on the topographs and depends on the direction of the diffraction vector. Secondly, unidentified point-like objects are visible among the gas voids. Finally, dislocations are associated not only with voids but also with groups of voids located in a certain configuration. The fact that the dominant slip system of dislocations is basal slip explains the change in their density on the topographs. Point-like contrasts can most probably be interpreted as molybdenum inclusions arising from the crucible and shaper.

The emission of dislocations from a void or group of voids in sapphire has not yet been quantified. So far, there is no quantitative explanation that takes into account the sizes of the voids. In the local region between rows 2 and 3 bounded by transverse row 5, groups of voids are visible that are not associated with dislocations. One of these groups is marked with an arrow (Fig. 3, *c*). As an example, we chose this group to calculate the size of voids.

Optical microscopy is commonly used for void sizing in sapphire crystals. However, when performing high magnification (about 100 times) optical microscopy, the reduced focus length is required to detect μm-sized gas inclusions, which limits the possibilities of visible light imaging to thin samples. The large thickness of the ribbon (about 1 mm) does not permit an accurate determination of the microvoid diameter. The PCI technique, which can be applied to both thin and thick specimens, enables a more complete description of sizes and shapes by solving the inverse problem. Therefore, in the present work, we used computer simulations to obtain the correct information from the images of voids.

Computer simulation

Phase-contrast images were recorded on a CCD and saved in Tag Image File Format (TIFF) 16 bit with a range of tag values from 0 to 65536. Analysis of the experimental image (2560×2160 pixels) taken at a distance of Z_1 = 14 cm showed that the tag values are in the range from 26616 to 43888. The group of selected voids was located on a fragment of 490×490 pixels. Within the fragment, the range of the tag values was even smaller: from 35738 to 41615.

The image contrast equals the difference between the maximal and minimal intensities of the image divided by the sum of these values. Therefore, the contrast was quite small: V = 0.076. At another distance Z_1 = 25 cm we got V = 0.114. That is, when the distance doubled, the contrast also doubled. In addition, as the distance increased the structure of the image changed slightly, namely, the areas of white (maximum) and black (minimum) colors.

Images of spherical voids have a simple structure consisting of a black ring around the edge and a light color in the middle of void. Outer diameter, black ring width, and void contrast increase with distance. For Z_1 = 25 cm, the diameter is 50 pixels. Given that the pixel size is 0.32 μm, we get 16 μm. Based on the model of a spherical pore with a diameter of 16 μm, we calculated images of the pore at a given distance Z_1. The calculation was performed using the XRWP2 (X-ray Wave Propagation 2D) program in the framework of the phase-contrast theory of three-dimensional objects. The program was written by V.G. Kohn using own ACL programming language [8], which is executed by the vkACL.jar interpreter elaborated with Java.

Wave propagation through an object is described by the transmission function, while propagation in free space is calculated according to the Huygens–Fresnel principle as the convolution of the wave function with the Fresnel propagator. The convolution is computed through the Fourier transform method. The fast Fourier transformation (FFT) method was applied.

The simulations were carried out for fully coherent monochromatic radiation from a point source. The source size, non-monochromaticity and detector resolution were counted on the intensity level. It is often sufficient to compute the convolution of the two-dimensional intensity distribution on the detector with a Gaussian of a given width. The FWHM (full width at half maximum) of the Gaussian in both directions were equal to each other, but the values were fitted. Fig. 4 shows the result obtained under the following conditions: void diameter is 16 μm; distance Z_1 = 14 cm and 25 cm; photon energy 25 keV, FWHM 5 μm. The contrast values of the simulated images were 0.133 и 0.241. These contrasts are higher than the experimental ones but they show the same trends.

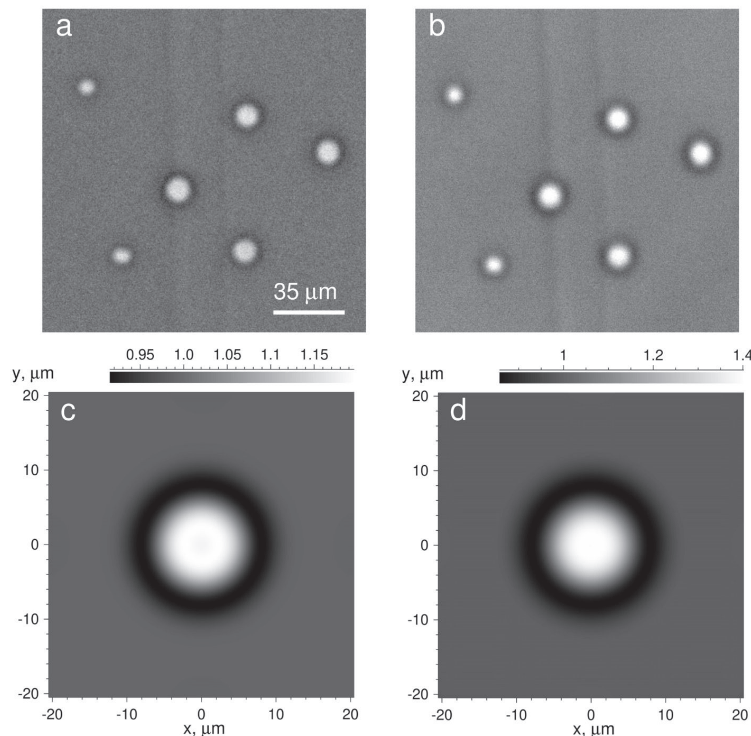

Fig. 4. Phase-contrast images of voids recorded at Z_1 = 14 cm (*a*) and Z_1 = 25 cm (*b*). Computed images of a void with a diameter of 16 μm at a distance of 14 cm (*c*) and 25 cm (*d*). The computation was made for the rightmost void in the experimental images

Summary

The combination of synchrotron radiation phase-contrast and Bragg-diffraction imaging makes it possible to visualize and characterize defects in profiled sapphire products, particularly in ribbons. Direct comparison of topographs and phase-contrast images reveals the relationships between gas voids and dislocations. The latter are present around the void, since the concentration of stresses at the edges of the void can promote dislocation emission. Computer simulations of phase-contrast images, performed using the author's computer program, solved the problem of determining the void size. Quantitative data (void size, void density, close distances between voids) will be used to build elastic models aimed at describing defect formation in basal-faceted sapphire ribbons.

REFERENCES

1. **Katyba G., Zaytsev K., Dolganova I., Shikunova I., Chernomyrdin N., Yurchenko S., Komandin G., Reshetov I., Nesvizhevsky V., Kurlov V.,** Sapphire shaped crystals for waveguiding, sensing and exposure applications, Prog. Cryst. Growth. Ch. 64 (2018) 133–151.

2. **Bruni F.,** Crystal growth of sapphire for substrates for high-brightness, light emitting diodes, Cryst. Res. Technol. 50 (1) (2015) 133–142.

3. **Denisov A., Molchanov A., Punin Yu., Krymov V., Müller G., Friedrich J.,** Analysis of the growth conditions of long single crystalline basal-plane-faceted sapphire ribbons by the Stepanov/EFG technique, J. Cryst. Growth. 344 (1) (2012) 38–44.

4. **Bunoiu O., Duffar Th., Nicoara I.,** Gas bubbles in shaped sapphire, Prog. Cryst. Growth. Ch. 56 (2010) 123–145.

5. **Kuandykov L., Bakholdin S., Shulpina I., Antonov P.,** Model of a block structure generation in basal-faceted sapphire ribbons, J. Cryst. Growth. 275 (1-2) (2005) e625–e631.

6. **Snigirev A., Snigireva I., Kohn V., Kuznetsov S., Schelokov I.,** On the possibilities of x-ray phase contrast microimaging by coherent high-energy synchrotron radiation, Rev. Sci. Instrum. 66 (12) (1995) 5486–5492.

7. **Argunova T., Kohn V.,** Problems with evaluation of micro-pore size in silicon carbide using synchrotron x-ray phase contrast imaging, Materials. 15 (2022) 856(1–7).

8. **Kohn V.,** 2006. URL: http://kohnvict.ucoz.ru/acl/acl.htm Accessed Oct. 19, 2022.

THE AUTHORS

ARGUNOVA Tatiana S.
argunova@mail.ioffe.ru
ORCID: 0000-0003-2085-6183

KRYMOV Vladimir M.
v.krymov@mail.ioffe.ru

KOHN Victor G.
kohnvict@yandex.ru
ORCID: 0000-0003-4332-9896

Received 26.10.2022. Approved after reviewing 08.11.2022. Accepted 07.12.2022.

© Peter the Great St. Petersburg Polytechnic University, 2023